Article

De novo design of chemical stability near-infrared molecular probes for high-fidelity hepatotoxicity evaluation in vivo

Dan Cheng, Juanjuan Peng, Yun Lv, Dongdong Su, Dongjie Liu, Mei Chen, Lin Yuan, and XiaoBing Zhang

J. Am. Chem. Soc., **Just Accepted Manuscript** • DOI: 10.1021/jacs.9b01374 • Publication Date (Web): 22 Mar 2019

De novo design of chemical stability near-infrared molecular probes for high-fidelity hepatotoxicity evaluation *in vivo*

Dan Cheng[†], Juanjuan Peng[‡], Yun Lv[†], Dongdong Su[§], Dongjie Liu[#], Mei Chen[#], and Lin Yuan*[,†], Xiaobing Zhang[†]

[†]State Key Laboratory of Chemo/Biosensing and Chemometrics, College of Chemistry and Chemical Engineering, Hunan University, Changsha 410082 (PR China)

[‡]State Key Laboratory of Natural Medicines, School of Basic Medical Sciences and Clinical Pharmacy, China Pharmaceutical University, Nanjing, Jiangsu, 211198, China.

[§]Department of Chemistry and Chemical Engineering, Beijing University of Technology, Beijing 100124, China.

[#]College of Materials Science and Engineering, Hunan University, Changsha 410082, China

Abstract: Near-infrared (NIR) fluorescence imaging technique is garnering increasing research attention due to various superiorities. However, most NIR fluorescent probes still suffer from false signals problem owing to their instability in the real application. Especially in a pathological environment, many NIR probes can easily be destroyed due to the excessive generation of highly reactive species and causing a distorted false signal. Herein, we proposed an approach for developing a new stable NIR dye platform with an optically tunable group to eliminate false signals using the combination of dyes screening and rational design strategy. The conception is validated by the construction of two high-fidelity NIR fluorescent probes (**NIR-LAP** and **NIR-ONOO$^-$**) sensing leucine aminopeptidase (LAP) and peroxynitrite (ONOO$^-$), the markers of hepatotoxicity. These probes (**NIR-LAP** and **NIR-ONOO$^-$**) were demonstrated to sensitively and

accurately monitor LAP and $ONOO^-$ (detection limit: 80 mU/L for LAP and 90 nM for $ONOO^-$), thereby allowing to precisely evaluate drug induced hepatotoxicity. In addition, based on the fluctuation of LAP, the therapeutic efficacy of six hepatoprotective medicines for acetaminophen-induced hepatotoxicity was analyzed *in vivo*. We anticipate the high-fidelity NIR dye platform with an optically tunable group could provide a convenient and efficient tool for the development of future probes applied in the pathological environment.

Introduction

Fluorescence imaging technique has been an effective approach for detecting various bioanalytes in living cells and animals with the advantages of simplicity, sensitivity, and noninvasiveness.[1-8] A mass of fluorescent probes have been applied in monitoring bioanalytes activity, diagnosis, and even surgical navigation.[9-12] Among the activatable fluorescent probes, near-infrared (NIR) molecules are more popular due to the high tissue penetration depth and low auto-fluorescence from biosystems.[13-17] Thus, NIR fluorescent probes for tracking special analytes changes in living system in real-time are highly desirable, which might facilitate the investigation of their functions and associated disease diagnosis. Although many excellent works have been reported for various application by using NIR fluorescent probes,[18-20] the development of suitable probes for accurate detection of target analytes remains challenging due to the inherent limitations of classic NIR dyes. Recently, our and other groups have reported some new type of fluorescent dyes with optically tunable group,[21-24] which have been used to develop NIR probes with improved signal-to-background ratio by various groups.[25-27] However, most of the NIR probes are still faced with false signals problem.[26] There are two main causes of false signals: 1) poor

selectivity, interfering from multiple biomolecular in the complicated biological environment; 2) poor stability, decomposing by highly reactive species or nucleophiles in living system. In particular, if the selectivity of a fluorescent probe is poor, it will recognize the analogs of the target analyte and cause false-positive signal. On the other hand, if a fluorescent probe/dye has poor stability, it is easily cleaved by biological relevant molecules (nucleophilic or oxidative species) before or after the analyte is recognized in biological medium,[28,29] also resulting in false-negative signal (Figure 1A). So far, most efforts have focused on improving the selectivity of probes themselves to solve the false signal. However, less effort has been made to enhance the chemical stability of probes/fluorophores against highly reactive species and nucleophiles *in vivo*. Therefore, rational design of highly stable NIR fluorescent probes with high performance to attain accurate detection and avoid false signals toward target analyte is essential for practical application.

Generally, in the clinic pathological environment, there is a higher concentration of highly active species than the normal states. Thus, the NIR probes themselves easily been damaged by these species before responding with target analytes and resulted in false signals. Therefore, it is a higher demand for the stability of NIR probes. Liver injury, such as drug-induced liver injury (DILI), is a representative pathological example. DILI is a major public health problem affecting patients, pharmacist, medicine developers, and medicine regulatory agencies. Most DILI occurs in accidental or intentional overdose of medicines, and DILI has become one of the major reasons of acute hepatic injury.[30-33] Recent biomedical studies have demonstrated that highly reactive oxygen/nitrogen species (ROS/RNS), such as $ONOO^-$ are over produced in mitochondria up to high level after overdose of medicines, leading to severe hepatotoxicity.[25,34-37] In addition, the activity of the enzyme, leucine aminopeptidase (LAP), is greatly increased during hepatic

dysfunction compared to the normal states.[38] Thus, $ONOO^-$ and LAP can be used as early diagnostic indicators for drug-related liver disease.[38-41] However, most developed fluorescent probes for DILI suffered from the false signal due to the degeneration of the probes caused by high concentrations of ROS/RNS and nucleophiles in liver injury *in vivo*. Therefore, we intend to construct $ONOO^-$ and LAP NIR probes to validate our design conception and the DILI detection was chosen as the disease model for developing probe.

In this work, screening combined with rational design method was applied for the development of NIR fluorescent probes, and the effectiveness of this approach has been proved by our previous work[4]. We collected a series of NIR fluorescent dyes including DCM dyes, BODIPY dyes, cyanine dyes, squaric acid dyes and benzopyran dyes, *etc.,* and tested their stability toward various highly reactive species and screened out a stable NIR fluorophore. Then, working as a platform, two kinds of high-fidelity fluorescent probes (**NIR-LAP** and **NIR-ONOO$^-$**) for LAP and $ONOO^-$ were constructed, respectively. Both probes showed high sensitivity (detection limit is 80 mU/L for LAP and 90 nM for $ONOO^-$) and prominent stability to coexisted ROS and RNS. The effectiveness of probes was proved by detection of cellular mitochondrial LAP and $ONOO^-$ and used to visualize small fluctuations of LAP and $ONOO^-$ in medicine-induced hepatotoxicity. Finally, our probes were successfully used to monitor the effectiveness of remediation medicines for paracetamol (APAP)-induced hepatotoxicity. Thus, the combined screening and rational design approach provide a convenient and efficient strategy for high-fidelity NIR probes to reform their stability and sensitivity in analytes sensing.

Results and Discussion

Design and synthesis of probes. Initially, two commonly used dyes were designed and

synthesized as NIR probes, **DCM-ONOO$^-$** and **HD-ONOO$^-$** (Figure 1B). They can be used to detect $ONOO^-$, based on the combination of **DCM** and **HD-NH$_2$** dyes and α-keto acid, a well-known $ONOO^-$ reaction site that can be successfully carried out under physiological conditions.[40,42] However, the spectral results showed that both **DCM-ONOO$^-$** and **HD-ONOO$^-$** could not produce a positive signal after responding to $ONOO^-$ (Figure 1C, S1 and S2). Especially, for **HD-ONOO$^-$**, when it reacted with a lower concentration of $ONOO^-$, the intensity of emission spectra slightly increased (Figure S2), whereas the intensity rapidly decreased with a higher concentration of $ONOO^-$ (Figure 1C). For this phenomenon, we supposed that the probe (**HD-ONOO$^-$**) and the dyes (**DCM** and **HD-NH$_2$**) are unstable in the presence of $ONOO^-$ and are oxidative cleaved by $ONOO^-$ (Scheme S1-2). At the same time, there was a competitive relationship between the recognition and destruction of probes (Scheme S1). The spectral results (Figure 1D, E) and ESI-MS (Figure S3 and S4) confirmed our hypothesis that the dyes were decomposed by $ONOO^-$ and caused false-negative fluorescent signals. To solve the false signals problem and improve the sensitivity of fluorescent probes in practical applications, we thus intend to develop highly stable and selective dyes for $ONOO^-$/LAP based on a rational design strategy and screening approach. The designed NIR dye was further combined with the $ONOO^-$/LAP reaction sites and developed into specific fluorescent probes.

The synthesized or purchased 23 kinds of NIR dyes serve as the potential candidate dyes (Scheme S3). Their stability toward various oxidants and nucleophiles, such as nitric oxide (NO), $ONOO^-$, superoxide anion radical ($O_2^{\bullet-}$), hydrogen peroxide (H_2O_2), hydrogen persulfide (H_2S_2), sulfite (SO_3^{2-}), hydrogen sulfide (H_2S), was evaluated in an aqueous solution (PBS/EtOH =8/2, pH 7.4). As shown in Figures 2A, S5-28 and Tables S1-23, among the 23 dyes, only the

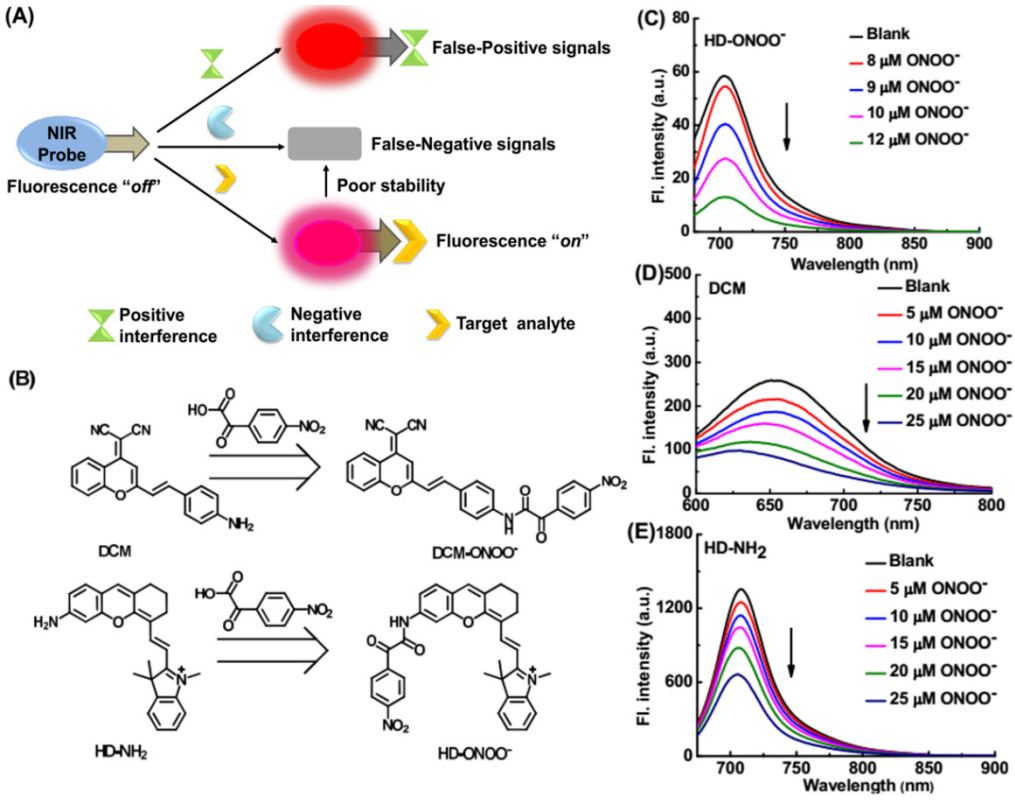

Figure 1. (A) Proposed reasons of the generation of false fluorescence signals for NIR fluorescent probe. (B) Design and structure of **DCM-ONOO**$^-$ and **HD-ONOO**$^-$. (C) Fluorescence spectra of **HD-ONOO**$^-$ with increasing concentration of $ONOO^-$ (8-12 μM). (D) Fluorescence spectra of **DCM** with increasing concentration of $ONOO^-$ (0-25 μM). (E) Fluorescence spectra of **HD-NH$_2$** with increasing concentration of $ONOO^-$ (0-25 μM). All spectra were measured in PBS/EtOH (v/v, 8/2, pH 7.4) buffer solution.

fluorescence intensities of compounds **2** and **10** were almost constant in the presence of various oxidants or nucleophiles, indicating that compounds **2** and **10** have high stability and can be used for detection. Fluorescent probes with NIR emission (650-900 nm) have low autofluorescence and high penetration depth to bio-sample. Due to the shorter emission wavelength (Figure S29), compound **2** is limited for *in vivo* imaging applications despite its relatively high stability (Figure 2A and S7). In addition, thanks to the introduction of a benzoic acid group into the destroyed site of **HD-NH$_2$** to prevent attack by other species, we supposed that compound **10** has a more stable conjugated system than **HD-NH$_2$**. There exists the similar relationship of chemical stability

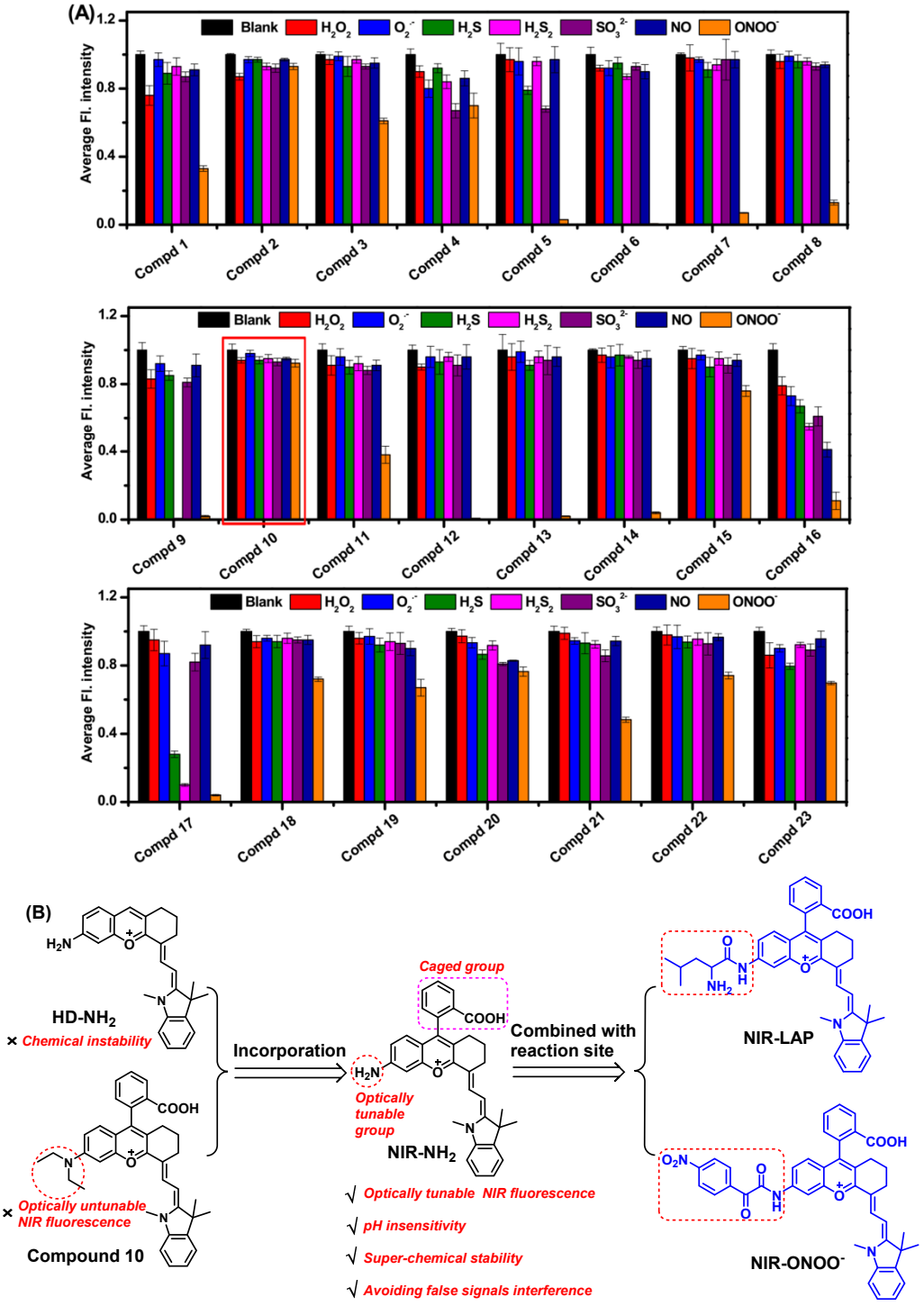

Figure 2. (A) Fluorescence intensities of dyes **1**-**23** (5 μM, structure of dyes **1**-**23** are shown in Scheme S3) to various agents in an aqueous solution (PBS/EtOH = 8/2, pH 7.4) (25 μM for $ONOO^-$; 100 μM for H_2O_2, $O_2^{\bullet-}$, H_2S, NO; 150 μM for SO_3^{2-}; 50 μM for H_2S_2). The tested solution was kept at 37 ℃ for 20 min before the data was recorded. (B) Design and structure of compounds **NIR-NH$_2$**, **NIR-LAP** and **NIR-ONOO$^-$**.

between rhodamine B and pyronine dye (Figure S30), the only difference between their chemical

structures is what the former owns one more stable benzoic acid group than the later dye. Therefore, the compound **NIR-NH_2** was designed and synthesized by incorporation of compound **HD-NH_2** and compound **10** (Figure 2B), and as we all expect, the compound showed good stability to various biological relevant ROS/RNS (e.g. H_2O_2/$ONOO^-$) and nucleophiles (e.g. H_2S) (Figures S31-34). Accordingly, the compound **NIR-NH_2** with an optically tunable group was chosen as the chemically stable dye and constructed target probes through an amino protection/deprotection approach.[43-45] At the same time, the amino-protecting compound **NIR-NHCO** was synthesized and its stability was examined. It also showed high stability toward various species including $ONOO^-$ (Figures S35-38), indicating good stability of future amino-protected fluorescent probes. L-leucine and 4-nitrophenylglyoxylic acid can serve as the amino-protecting groups, meanwhile, their corresponding amide derivatives have been demonstrated that the protected amino groups can be released by LAP or $ONOO^-$, respectively.[15,40] Based on this, we designed and synthesized two NIR fluorescent "turn on" probes (**NIR-LAP** and **NIR-$ONOO^-$** (Figure 2B)).

Sensing properties of fluorescent probes to LAP and $ONOO^-$. First, we investigated the effect of probes on the detection of LAP or $ONOO^-$ by spectral analysis. Probe **NIR-LAP** initially showed strong absorption peaks at 608/657 nm with weak fluorescence ($\Phi < 0.01$) (Figure S39 and Figure 3A). As expected, after reaction with LAP (0-100 U/L), a red-shifted absorption to 622/670 nm with a color change from blue to light green (Figure 3A) was observed, and a gradual fluorescence enhancement at 703 nm ($\Phi = 0.28$) was accompanied. This change was produced by the formation of the amino-deprotected compound **NIR-NH_2**, which was verified by ESI-MS analysis (Figure S40). At different concentrations of LAP (0, 5, 10, 50, 100 U/L), the fluorescence

intensity of **NIR-LAP** (5 μM) reached the plateau within 40 min (Figure S41). It is worth noting that an around 13-fold fluorescence enhancement was observed and there was an obvious linear relationship with LAP concentration from 0.1 to 1 U/L with the detection limit of 80 mU/L (Figure S42). Furthermore, the Michaelis constant of **NIR-LAP** to LAP was determined to be 106 μM

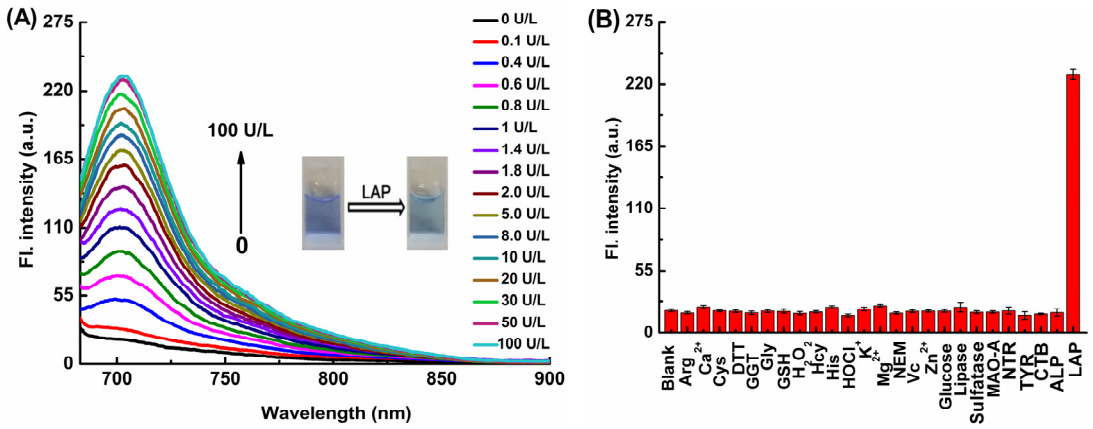

Figure 3. (A) Fluorescence emission spectra of **NIR-LAP** (5 μM) with increasing concentration of LAP (0-100 U/L). (B) Fluorescence intensity of **NIR-LAP** (5 μM) toward various analytes: LAP (50 U/L); GGT, TYR, CTB, ALP (100 U/L); lipase (10 mg/mL), sulfatase (1000 U/L), MAO-A, NTR (10 μg/mL); H_2O_2, HOCl (50 μM); Cys, DTT, GSH, Vc (1 mM); NEM (5 mM); Ca^{2+}, K^+, Mg^{2+}, Zn^{2+} (2.5 mM); Glucose (10 mM); other analytes (100 μM). All test solution was kept at 37 ℃ for 40 min in pH 7.4 PBS buffer solution before the data was recorded (λ_{ex} = 660 nm).

(Figure S43), indicating that **NIR-LAP** is sensitive and can monitor LAP with strong affinity, which can be compared to reported data (Table S24). Similarly, for probe **NIR-ONOO$^-$**, the concentration of $ONOO^-$ (0-15 μM) addition generated significant NIR fluorescence enhancement (7-fold) with color change (Figure S44) and a red-shifted absorption from 611/661 to 627/678 nm (Figure S45), thereby affording product **NIR-NH$_2$**. The reaction mechanism was also verified by ESI-MS analysis (Figure S46). There was a good linear correlation between fluorescence intensity and $ONOO^-$ concentrations, which was determined to be 9.0×10^{-8} M (Figure S47) for the

detection limit, and it was also compared to the published NIR fluorescent $ONOO^-$ probes (Table S25). These results indicate that **NIR-ONOO$^-$** display high sensitive respond to $ONOO^-$ and can be applied to image trace amount of $ONOO^-$ in living cells. The selectivity and specificity of **NIR-LAP** for LAP and **NIR-ONOO$^-$** for $ONOO^-$ in the presence of various biological species were examined, including ROS/RNS ($O_2^{\bullet-}$, HOCl, H_2O_2, BuOOH, HNO and NO_2^-), reactive sulfur species (RSS: HSO_3^-, SO_3^{2-}, H_2S, H_2S_2, Cys, Hcy, GSH, and DTT), cations and anions (K^+, Na^+, Mg^{2+}, Ca^{2+}, Zn^{2+}, Fe^{2+}, Cu^{2+}, and CH_3COO^-), biomolecules (vitamin C, glucose, arginine, histidine, glycine and N-ethylmaleimide) and some enzyme species (GGT, lipase, sulfatase, MAO-A, nitroreductase (NTR), tyrosinase (TYR), Cathepsin B (CTB), alkaline phosphatase (ALP)). As shown in Figure 3B and S48, there are slight fluorescence intensity changes towards other analytes. However, when **NIR-LAP** or **NIR-ONOO$^-$** was incubated with LAP or $ONOO^-$, the fluorescence was significantly enhanced, indicating that these probes have excellent selectivity for LAP or $ONOO^-$ over other interference species in physiological conditions. In addition, H_2O_2 is a known interfering substance that affects the detection of $ONOO^-$,[4] so we performed a detailed titration experiment on H_2O_2 for **NIR-ONOO$^-$**. When high concentration (up to 1 mM) of H_2O_2 was added, no obvious fluorescence response of **NIR-ONOO$^-$** was observed (Figure S49). The results confirmed the superior selectivity of **NIR-ONOO$^-$** from H_2O_2, probably because the nucleophilicity of $ONOO^-$ is much stronger than that of H_2O_2.[4] Moreover, the temperature optimization results showed that the optimal temperature for LAP detection was 37 ^oC, which is the optimum temperature of the human body (Figure S50). And the pH effect results showed that both **NIR-LAP** and **NIR-ONOO$^-$** for LAP or $ONOO^-$ detection were in the range of pH 6 to 9 (Figure S51). Furthermore, we also tested the photostability of probes **NIR-LAP** and

NIR-ONOO$^-$ (Figure S52), exhibiting relatively good photostability compared to classical NIR dyes Cy5 and Mito-Tracker Deep Red, respectively. All results indicated the potential outstanding performance of **NIR-LAP** and **NIR-ONOO$^-$** for detecting LAP and ONOO$^-$ in physiological conditions.

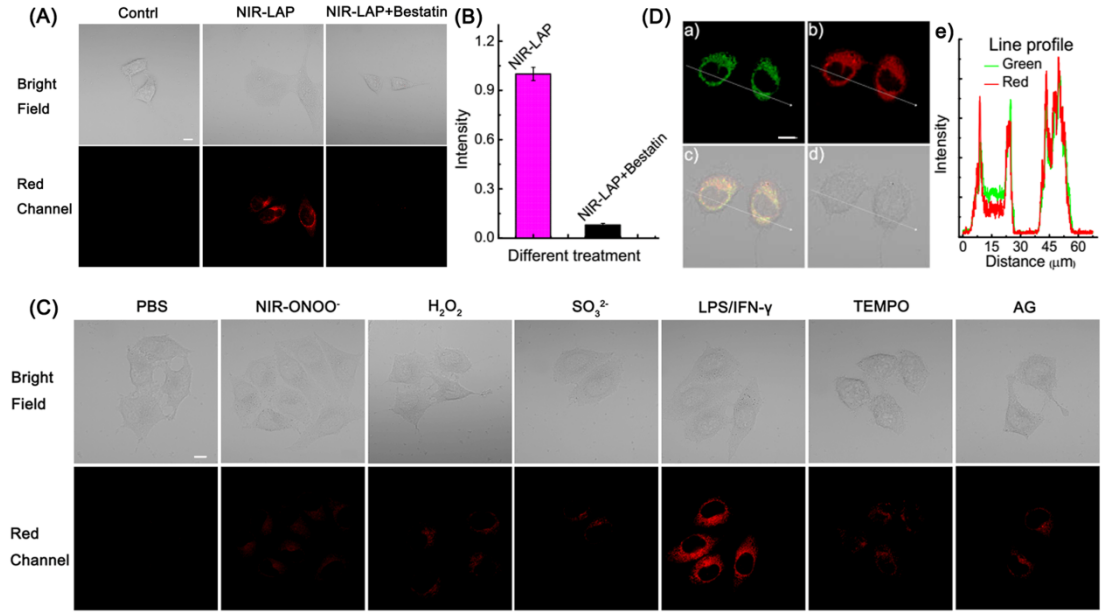

Figure 4. (A) Confocal images of LAP in HepG2 cells. First column, images of the cells without any treatment; Second column, images of cells pre-incubated with **NIR-LAP** (5 μM) for 20 min; Third column, images of cells pre-incubated with bestatin (100 μM) for 1 h then treated with **NIR-LAP** (5 μM) for another 20 min. (B) Fuorescence intensity in Figure 4(A). (C) Confocal images of ONOO$^-$ in HepG2 cells. First column, images of cells without any treatment; Second column, images of cells incubated with **NIR-ONOO$^-$** (5 μM) for 20 min; Third-fourth column, images of cells pretreated with **NIR-ONOO$^-$** (5 μM) for 20 min then incubated with H_2O_2 (100 μM) (third column) or SO_3^{2-} (100 μM) (fourth column) for another 30 min; Fifth column, images of cells were pre-stimulated with LPS (1 μg/mL) and IFN-γ (50 ng/mL) for 12 h and then incubated with **NIR-ONOO$^-$** (5 μM) for 20 min; Sixth-seventh column, images of cells co-incubated with LPS (1 μg/mL)/IFN-γ (50 ng/mL) and TEMPO (300 μM) (sixth column) or aminoguanidine (AG, 5 mM) (seventh column) for 12 h and then further treated with **NIR-ONOO$^-$** (5 μM) for 20 min. (D) The colocalization of **NIR-LAP** in HepG2 cells (Pearson's correlation coefficient (r) = 0.82). Green channel: Mito-Tracker Green (1 μM) stain (λ_{ex}= 488 nm, λ_{em} = 500-550 nm); red channel: **NIR-LAP** (5 μM) stain (λ_{ex} = 640 nm, λ_{em} = 663-738 nm); yellow: merged signal. Scale bar: 10 μm.

Imaging of cellular LAP and ONOO$^-$. Encouraged by the excellent properties of **NIR-LAP** and

NIR-ONOO$^-$ in vitro, their capabilities for detecting LAP and ONOO$^-$ in living cells were examined. First, standard MTT assays showed low cytotoxicity of **NIR-LAP** and **NIR-ONOO$^-$** (Figure S53), exhibiting the good biocompatibility of the probes. The efficacy of **NIR-LAP** and **NIR-ONOO$^-$** to visualize LAP and ONOO$^-$ in living cells was then evaluated. HepG2 cells displayed almost no emission signal in the absence of **NIR-LAP** (Figure 4A). However, there is a remarkable cellular fluorescence enhancement in the presence of **NIR-LAP**, indicating that the probe has good cell permeability. To further demonstrate the selectivity of the probe, cells were pre-incubated with bestatin, a specific inhibitor of LAP,[46] and then treated with **NIR-LAP**. The cells exhibited a large degree of degenerative fluorescence due to a decrease in intracellular LAP level (Figure 4B), demonstrating that probe **NIR-LAP** was well suited for the specific monitoring of endogenous LAP in living cells.

Next, we evaluated the capability of **NIR-ONOO$^-$** for endogenous ONOO$^-$ detection. Cellular selectivity is always a concern. In order to avoid potential interference from other biological species, the selectivity of **NIR-ONOO$^-$** to ONOO$^-$ was first confirmed in living cells. HepG2 cells themselves did not show fluorescence when excited with a wavelength of 640 nm (Figure 4C). When treated with **NIR-ONOO$^-$**, negligible fluorescence was observed. However, notably enhanced fluorescence was observed when the **NIR-ONOO$^-$** loaded cells were pre-incubated with lipopolysaccharide (LPS) and interferon-gamma (IFN-γ), which stimulated endogenous ONOO$^-$ production.[47] In contrast, there was almost no noticeable fluorescence enhancement when the cells pretreated with H_2O_2 or SO_3^{2-}, the possible strong interfering oxidant and nucleophiles. Moreover, aminoguanidine (AG, a nitric oxide synthase inhibitor)[48] or 2,2,6,6-tetramethylpiperidine-N-oxyl (TEMPO, a specific superoxide scavenger)[48] were used to

inhibit endogenous $ONOO^-$ generation. Significant fluorescence reduction was observed from TEMPO and AG-treated cells, clearly indicating that strong fluorescence from red channel of activated HepG2 cells is attributed to the generation of $ONOO^-$ (Figure 4C). These results demonstrated that **NIR-ONOO$^-$** could specifically detect and image endogenous $ONOO^-$ with high anti-interference ability in living cells. In addition, there are gradually enhanced red fluorescence in HepG2 and HeLa cells with dose-dependent SIN-1, an $ONOO^-$ donor (Figures S54 and S55), implying that **NIR-ONOO$^-$** was suitable for specific and semi-quantitative monitoring of exogenous $ONOO^-$.

To determine the intracellular localization of **NIR-LAP** and **NIR-ONOO$^-$**, we conducted costaining experiments. The fluorescence image of **NIR-LAP** excellent overlaps with the green fluorescence of Mito-Tracker Green ($r = 0.82$, Figure 4D) in HepG2 cells, proving the potent mitochondria-targetable ability of probe **NIR-LAP**. Probe **NIR-ONOO$^-$** was also mainly located in mitochondria ($r = 0.87$), while the overlap efficiency with the image of Lyso-Tracker was low (Figure S56). The distribution tendency can be explained by the fact that a compound with positive charge significantly increases the localization in mitochondria.[49,50]

Screening and imaging of LAP and $ONOO^-$ in DILI model. As a proof-of-concept experiment, we explored the performance of **NIR-LAP** and **NIR-ONOO$^-$** in DILI model cells.[51,52] Overdose acetaminophen (APAP) has been reported to cause acute liver injury, and during this process, LAP or $ONOO^-$ is produced and eventually leads to cell death.[40,41] First, we evaluated the production of LAP in APAP stimulated cells by probe **NIR-LAP**. Cells incubated with **NIR-LAP** showed red fluorescence (Figure 5A), indicating the existence of intrinsic LAP. When cells were preincubated with APAP and then further treated with **NIR-LAP**, the fluorescence intensity steadily enhanced

with the increased concentration of APAP (Figure 5A and B). This demonstrated that **NIR-LAP** can monitor the fluctuation of intracellular LAP after APAP stimulation. To further confirm the effectiveness of **NIR-LAP** for LAP monitoring, N-acetylcysteine (NAC), a medicine approved by the U.S. Food and Medicine Administration (FDA),[53] was used to remedy APAP-induced liver injury. A noticeable fluorescence depression was observed after the addition of NAC to HepG2 or L02 cells (Figure 5A, B and Figure S57). We hypothesized that it may be because cells with self-repairing function are able to achieve a redox balance after oxidative stress, which leads to the regulation of LAP levels. In addition, bestatin, a LAP reactivity inhibitor[46], pre-incubated L02 cells displayed a notably diminish in the fluorescence intensity (Figure S57). Taken all, these results strongly confirm the capacity of probe **NIR-LAP** for LAP detection and imaging in cells. Then, probe **NIR-ONOO$^-$** was used to screen and image DILI with another biomarker, ONOO$^-$. HepG2 cells were preincubated with different concentrations of APAP and then further treated with **NIR-ONOO$^-$** (5 μM) for 20 min. It is clear that a gradual increase in fluorescence signal confirms the effectiveness of probe **NIR-ONOO$^-$** to monitor ONOO$^-$ variation during APAP-induced hepatotoxicity (Figure S58). In addition, endogenous LAP and ONOO$^-$ activities were also analyzed by flow cytometry in APAP-induced liver injury. The fluorescence intensity enhanced significantly after treatment of HepG2 cells with various concentrations of APAP (0, 100, 500 and 1000 μM) (Figure 5C). An increase in fluorescence was also observed for ONOO$^-$ detection by probe **NIR-ONOO$^-$** in APAP-stimulated cells (Figure S59). In summary, both **NIR-LAP** and **NIR-ONOO$^-$** were able to accurately detect the fluctuation of intracellular LAP and ONOO$^-$ in APAP-induced liver injury. We further employed them to investigate the association of hepatotoxicity therapy and LAP or ONOO$^-$ level in living cells and mouse.

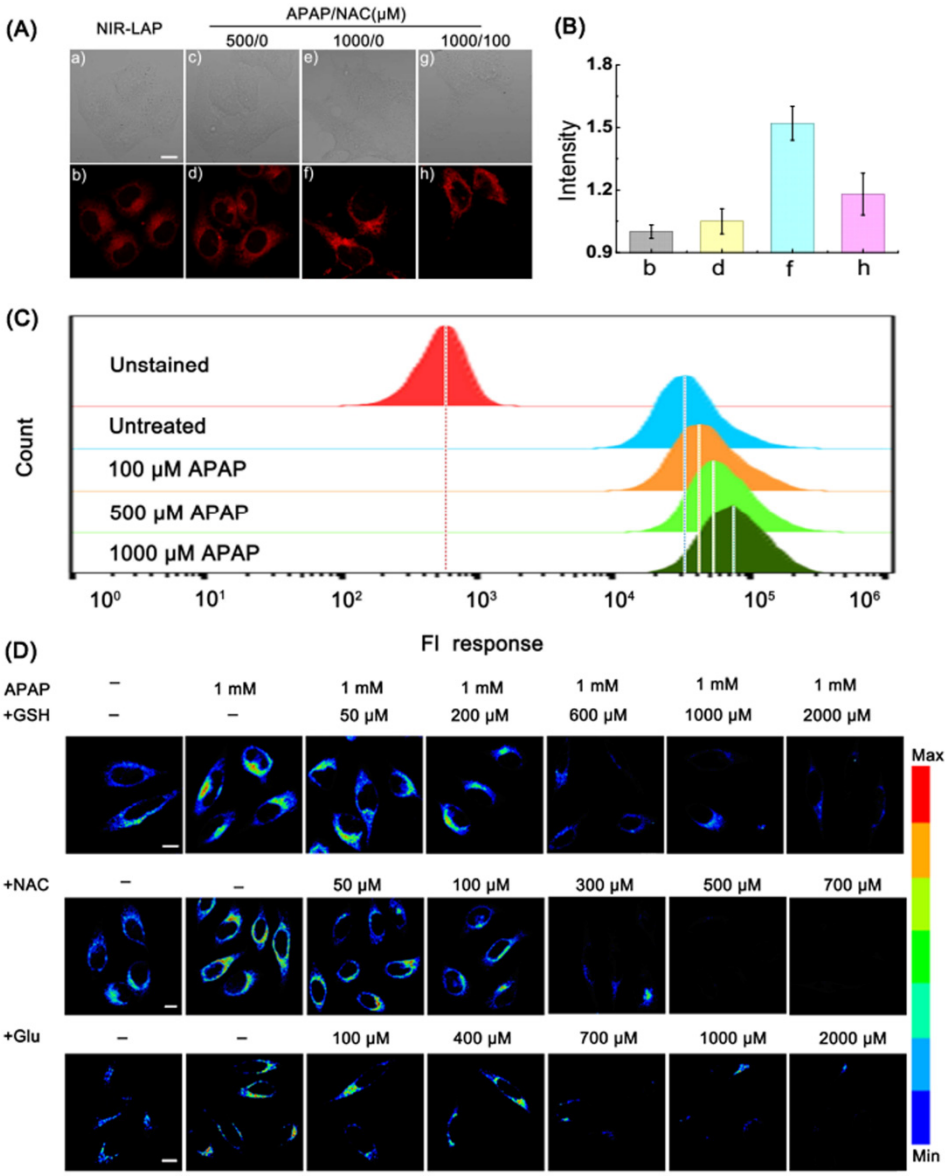

Figure 5. (A) Confocal images of LAP in HepG2 cells treated with only probe **NIR-LAP** (5.0 μM) or pretreated with NAC (0 and 100 μM) for 1 h before co-incubated with APAP (500 or 1000 μM) for 12 h (λ_{ex} = 640 nm, λ_{em} = 663-738 nm; Scale bar: 10 μm). (B) Relative fluorescence intensity in Figure 5(A). (C) The flow cytometric analysis of intact HepG2 cells and HepG2 cells-loaded **NIR-LAP** treated with APAP (0-1000 μM). The X-axis is FL-7 channel that captured the fluorescence of **NIR-LAP** (λ_{ex}= 633 nm, λ_{em}= 725 nm). (D) HepG2 cells treated with probe **NIR-LAP** (5.0 μM) or pretreated with different concentration of GSH (0-2000 μM), NAC (0-700 μM) and Glu (0-2000 μM) for 1 h before co-incubated with APAP (1 mM) for 12 h (λ_{ex} = 640 nm, λ_{em} = 663-738 nm; Scale bar: 10 μm). (-) represents the cells were untreated with medicines.

Monitoring the therapy of hepatoprotective medicine after APAP-induced hepatotoxicity in living cells. The liver is an important organ of body, so many healthcare and hepatoprotective

medicines have been developed to protect the liver after DILI. In order to verify the safety of healthcare and the effectiveness of medicines, it is essential to develop probes with high performance for hepatotoxicity screening for the pharmaceutical industry during medicine development. Our probes were applied to monitor the protective effects of the hepatoprotective medicines through a liver detoxification mechanism. NAC was chosen as a reference medicine and experiments were performed in live HepG2 cells. Glutathione (GSH) and Glucurolactone (Glu) were selected as candidate hepatoprotective medicines for DILI.[30,40] Cells pretreated with **NIR-LAP** showed increased fluorescence intensity after exposure to APAP compared to untreated cells (Figure 5D). After further treatment with NAC, GSH or Glu, the intracellular fluorescence intensity gradually decreased. And the degree of reduction was proportional to the concentration of NAC, GSH or Glu (Figure 5D). By comparing the changes in fluorescence intensity induced by NAC, GSH or Glu, when LAP is used as a therapeutic indicator of hepatotoxicity, NAC may be superior to GSH and Glu as an antidote to APAP toxicity. It can prevent the increase of LAP more effectively, probably because NAC has better oxidation resistance. In addition, when another biomarker, $ONOO^-$, was used as an indicator of hepatotoxicity therapy, GSH performed better than NAC and Glu. This may be because the intake of GSH helps to enhance liver detoxification and reduce liver damage caused by acetaminophen (Figure S60). All of these screening and imaging results indicated that the constructed probes, **NIR-LAP** and **NIR-ONOO$^-$**, were effective in assessing the protective effects of medicines after DILI.

Screening remediation of APAP-induced hepatotoxicity *in vivo.* In order to confirm the high-fidelity utility of our probes, we evaluated the stability of our designed compounds **NIR-NH$_2$** and **NIR-ONOO$^-$** through compared with the control probe **HD-ONOO$^-$** and conventional dyes in

hepatotoxicity (Figure S61 and S62) *in vivo*. Our probe has a superior performance in terms of resisting destruction from APAP stimulated hepatotoxicity conditions. Then, encouraged by the results of above studies, the probes were finally applied to *in vivo* imaging and screening for hepatoprotective medicines against APAP-induced liver injury.

Probe **NIR-LAP** was selected as the representative probe for assessing the hepatotoxicity and remediation of APAP-induced hepatotoxicity *in vivo*. Firstly, the cytotoxicity of the probe was evaluated *in vivo*. After intravenous injection with probe **NIR-LAP** for one or two days, ALT and AST levels in serum and the histological evaluation of major organs showed good biocompatibility of the developed probe (Figure S63). In addition, we also investigated the biodistribution of the probe *in vivo*, and the results indicated that **NIR-LAP** was mainly accumulated in the liver after intravenously administrated to BALB/c mice (Figure S64). The remediation of APAP-induced hepatotoxicity experiments was then evaluated. NAC, GSH, Glu and two traditional liver injury remediation medicines,[54,55] biphenyldicarboxylate (DDB) and ursodeoxycholic acid (UDCA) were chosen for remediation of hepatotoxicity. First, 45 min after intraperitoneal injection of APAP (300 mg/kg), **NIR-LAP** was injected via tail vein, and anesthetized to acquire sequential images at different time points. The obtained images showed significant fluorescence enhancement in the liver area from 80 min to 140 min after administration of probe **NIR-LAP** (Figure 6A). Above results confirmed that **NIR-LAP** can be used for *in vivo* hepatotoxicity detection. Mice were then pretreated with various hepatoprotective medicines, after 1 h and then treated with APAP to induce liver injury. Using probe **NIR-LAP**, a remarkable fluorescence reduction was observed compared to mice receiving only APAP (Figure 6A), indicating that these medicines act to APAP-induced liver injury in mice. Furthermore,

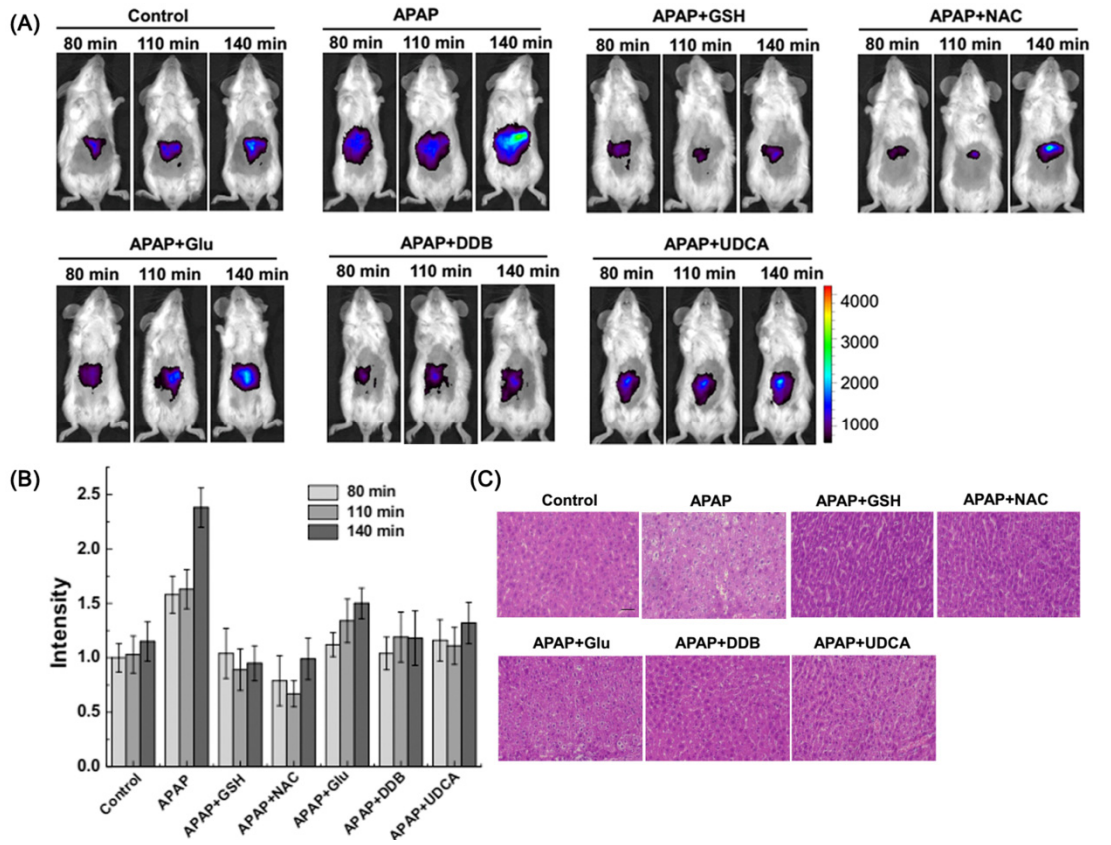

Figure 6. (A) Representative images of BALB/c mice receiving saline (Control), APAP (300 mg kg^{-1}, intraperitoneally) alone, or with GSH (200 mg kg^{-1}, intravenously), NAC (150 mg kg^{-1}, intravenously), Glu (200 mg kg^{-1}, intravenously), DDB (200 mg kg^{-1}, intraperitoneally), UDCA (20 mg kg^{-1},intraperitoneally), followed by **NIR-LAP** (60 μL, 100 μM, intravenously) (λ_{ex} = 640 nm, λ_{em} = 695-770 nm). (B) Relative fluorescence intensity in Figure 6 (A). Data are expressed as mean ± SD of three experiments. (C) H&E staining of liver tissues from mice treated with APAP only or treated with APAP and different hepatoprotective medicines for 300 min. Scale bar: 100 μm.

quantitative data within the liver region also proved the remediation effect of hepatoprotective medicine following APAP-induced hepatotoxicity (Figure 6B). Glu and UDCA were relatively ineffective in reducing hepatotoxicity due to the different pharmacological effects. It can be explained that the antioxidant capability of these medicines can offset the APAP-induced liver oxidative stress, resulting in a decrease in LAP production in mice.[53-56] These results indicated that

our probes can be used for medicine screening and remediation hepatotoxicity imaging *in vivo*. Moreover, histological analysis of liver tissues was performed to identify the different histological changes, such as cellular shrinkage or enlargement of the cell nucleus (Figure 6C). The results were consistent with the fluorescence results that liver tissues of mice treated with hepatoprotective medicines were closer to the normal state, while the vacuolization of the cells was observed from the injured liver tissues of the APAP injected mice. This means that our probes can monitor the effects of liver protection medicines against APAP-induced hepatotoxicity. Additionally, *ex vivo* imaging of each organ further confirmed the different liver hepatoprotective effects of these remediation medicines on APAP-induced liver injury (Figure S65). Taken all, the results confirmed our probes had high stability and sensitivity without interference from false signals. And these small fluorescent probes were first used to evaluate the curative effect of hepatoprotective in DILI process in living animals. In summary, the results indicated that **NIR-LAP** can monitor the drug-induced hepatotoxicity *in vivo*, and the liver protective effect of remediation medicines for DILI. The probes might serve as effective tools for investigating the pathology and therapeutic mechanisms of hepatotoxicity.

Conclusion

In summary, by the rational design of NIR dye platform with an optically tunable group based on the approach, we reported two new high-fidelity fluorescent probes **NIR-LAP** and **NIR-ONOO$^-$** for accurate, sensitive and selective detection of DILI with reduced false negative signals for the first time. These probes provided low detection limits for LAP (80 mU/L) or $ONOO^-$ (90 nM). Thanks to the high stability and selectivity under physiological conditions, our probes can detect small fluctuations of LAP or $ONOO^-$ in living cells. More importantly, these

fluorescent probes assessing the liver protective effects of hepatoprotective medicine in living animals was achieved. In a word, such novel NIR dye platform with an optically tunable group can readily be extended to develop other NIR fluorescent probes for different target analytes by simply changing the recognition site of dye, which could effectively avoid false signals and realize high-fidelity imaging in living system. Our work may offer a new method for future NIR fluorescent probes designs in biological applications such as medicine evaluation and therapy.

ASSOCIATED CONTENT

Supporting Information

Experimental details for experimental methods, dyes/probes synthesis, additional optical spectrum and imaging data. This material is available free of charge via the Internet at http://pubs.acs.org.

AUTHOR INFORMATION

Corresponding Author

* Email: lyuan@hnu.edu.cn

Notes

The authors declare no competing financial interest.

ACKNOWLEDGMENT

The work was supported by NSFC (21622504, 21877029, 21735001, 81701766), the Science and Technology Project of Hunan Province (2017RS3019) and China Postdoctoral Science Foundation (2018M642968). Compound **7**[57] was provided as a gift sample by Prof. Wei Guo (Shanxi University).

Reference

(1) Peng, T.; Yang, D. HKGreen-3: A Rhodol-Based Fluorescent Probe for Peroxynitrite. *Org. Lett.* **2010**, *12*, 4932-4935.

(2) Peng, T.; Wong, N.-K.; Chen, X.; Chan, Y.-K.; Ho, D. H.-H.; Sun, Z.; Hu, J. J.; Shen, J.; El-Nezami, H.; Yang, D. Molecular Imaging of Peroxynitrite with HKGreen-4 in Live Cells and Tissues. *J.*

Am. Chem. Soc. **2014**, *136*, 11728-11734.

(3) Zhou, X.; Kwon, Y.; Kim, G.; Ryu, J. H.; Yoon, J. A Ratiometric Fluorescent Probe Based on a Coumarin-Hemicyanine Scaffold for Sensitive and Selective Detection of Endogenous Peroxynitrite. *Biosens. Bioelectron.* **2015**, *64*, 285-291.

(4) Cheng, D.; Pan, Y.; Wang, L.; Zeng, Z.; Yuan, L.; Zhang, X.; Chang, Y.-T. Selective Visualization of the Endogenous Peroxynitrite in an Inflamed Mouse Model by a Mitochondria-Targetable Two-Photon Ratiometric Fluorescent Probe. *J. Am. Chem. Soc.* **2017**, *139*, 285-292.

(5) Sun, X.; Xu, Q.; Kim, G.; Flower, S. E.; Lowe, J. P.; Yoon, J.; Fossey, J. S.; Qian, X.; Bull, S. D.; James, T. D. A Water-Soluble Boronate-Based Fluorescence Probe for the Selective Detection of Peroxynitrite and Imaging in Living Cells. *Chem. Sci.* **2014**, *5*, 3368-3373.

(6) (a) Li, X.; Tao, R.-R.; Hong, L.-J.; Cheng, J.; Jiang, Q.; Lu, Y.-M.; Liao, M.-H.; Ye, W.-F.; Lu, N.-N.; Han, F.; Hu, Y.-Z.; Hu, Y.-H. Visualizing Peroxynitrite Fluxes in Endothelial Cells Reveals the Dynamic Progression of Brain Vascular Injury. *J. Am. Chem. Soc.* **2015**, *137*, 12296-12303. (b) Li, H.; Li, X.; Wu, X.; Shi, W.; Ma, H. Observation of the Generation of $ONOO^-$ in Mitochondria under Various Stimuli with a Sensitive Fluorescence Probe. *Anal. Chem.* **2017**, *89*, 5519-5525.

(7) Zhou, Z.; Wang, F.; Yang, G.; Lu, C.; Nie, J.; Chen, Z.; Ren, J.; Sun, Q.; Zhao, C.; Zhu, W.-H. A Ratiometric Fluorescent Probe for Monitoring Leucine Aminopeptidase in Living Cells and Zebrafish Model. *Anal. Chem.* **2017**, *89*, 11576-11582.

(8) Gong, Q.; Shi, W.; Li, L.; Ma, H. Leucine Aminopeptidase May Contribute to the Intrinsic Resistance of Cancer Cells toward Cisplatin as Revealed by an Ultrasensitive Fluorescent Probe. *Chem. Sci.* **2016**, *7*, 788-792.

(9) (a) Liu, H. W.; Chen, L. L.; Xu, C. Y.; Li, Z.; Zhang, H. Y.; Zhang, X. B.; Tan, W. H. Recent Progresses in Small-Molecule Enzymatic Fluorescent Probes for Cancer Imaging. *Chem. Soc. Rev.* **2018**, *47*, 7140-7180. (b) Li, X.; Gao, X.; Shi, W.; Ma, H. Design Strategies for Water-Soluble Small Molecular Chromogenic and Fluorogenic Probes. *Chem. Rev.* **2014**, *114*, 590-659.

(10) Zhang, J.; Chai X.; He X. P.; Kim, H. J., Yoon, J.; Tian, H. Fluorogenic Probes for Disease-Relevant Enzymes. *Chem. Soc. Rev.* **2019**, *48*, 683-722.

(11) Wang, L.; Zhang, J.; Kim, B.; Peng, J.; Berry, S. N.; Ni, Y.; Su, D.; Lee, J.; Yuan, L.; Chang, Y.-T. Boronic Acid: A Bio-Inspired Strategy To Increase the Sensitivity and Selectivity of Fluorescent NADH Probe. *J. Am. Chem. Soc.* **2016**, *138*, 10394-10397.

(12) (a) Miao, Q.; Yeo, D. C.; Wiraja, C.; Zhang, J.; Ning, X.; Xu, C.; Pu, K. Near-Infrared Fluorescent Molecular Probe for Sensitive Imaging of Keloid. *Angew. Chem. Int. Ed.* **2018**, *57*, 1256 -1260. (b) Lou, Z.; Li, P.; Han, K. Redox-Responsive Fluorescent Probes with Different Design Strategies. *Acc. Chem. Res.* **2015**, *48*, 1358-1368.

(13) Xu, K.; Chen, H.; Tian, J.; Ding, B.; Xie, Y.; Qiang, M.; Tang, B. A Near-Infrared Reversible Fluorescent Probe for Peroxynitrite and Imaging of Redox Cycles in Living Cells. *Chem. Commun.* **2011**, *47*, 9468-9470.

(14) (a) Yu, F.; Li, P.; Li, G.; Zhao, G.; Chu, T.; Han, K. A Near-IR Reversible Fluorescent Probe Modulated by Selenium for Monitoring Peroxynitrite and Imaging in Living Cells. *J. Am. Chem. Soc.* **2011**, *133*, 11030-11033. (b) Zhang, P.; Guo, Z.-Q.; Yan, C.-X.; Zhu, W.-H. Near-Infrared Mitochondria-Targeted Fluorescent Probe for Cysteine Based on Difluoroboron Curcuminoid Derivatives. *Chin. Chem. Lett.* **2017**, *28*, 1952-1956.

(15) Zhang, W.; Liu, F.; Zhang, C.; Luo, J.-G.; Luo, J.; Yu, W.; Kong, L. Near-Infrared Fluorescent Probe with Remarkable Large Stokes Shift and Favorable Water Solubility for Real-Time Tracking Leucine Aminopeptidase in Living Cells and In Vivo. *Anal. Chem.* **2017**, *89*, 12319-12326.

(16) Yuan, L.; Lin, W.; Zhao, S.; Gao, W.; Chen, B.; He, L.; Zhu, S. A Unique Approach to Development of Near-Infrared Fluorescent Sensors for in Vivo Imaging. *J. Am. Chem. Soc.* **2012**, *134*, 13510-13523.

(17) (a) Li, H.; Li, X.; Shi, W.; Xu, Y.; Ma, H. Rationally Designed Fluorescence •OH Probe with High Sensitivity and Selectivity for Monitoring the Generation of •OH in Iron Autoxidation without Addition of H_2O_2. *Angew. Chem. Int. Ed.* **2018**, *57*, 12830 -12834. (b) Yu, F.; Li, P.; Wang, B.; Han, K. Reversible Near-Infrared Fluorescent Probe Introducing Tellurium to Mimetic Glutathione Peroxidase for Monitoring the Redox Cycles between Peroxynitrite and Glutathione in Vivo. *J. Am. Chem. Soc.* **2013**, *135*, 7674-7680.

(18) Escobedo, J. O.; Rusin, O.; Lim, S.; Strongin, R. M. NIR Dyes for Bioimaging Applications. *Curr. Opin. Chem. Biol.* **2010**, *14*, 64–70.

(19) Yuan, L.; Lin, W.; Zheng, K.; He, L.; Huang, W. Far-Red to Near Infrared Analyte-Responsive Fluorescent Probes Based on Organic Fluorophore Platforms for Fluorescence Imaging. *Chem. Soc. Rev.* **2013**, *42*, 622-661.

(20) Guo, Z.; Park, S.; Yoon, J.; Shin, I. Recent Progress in the Development of Near-Infrared Fluorescent Probes for Bioimaging Applications. *Chem. Soc. Rev.* **2014**, *43*, 16-29.

(21) Yuan, L.; Lin, W.; Yang, Y.; Chen, H. A Unique Class of Near-Infrared Functional Fluorescent Dyes with Carboxylic-Acid-Modulated Fluorescence ON/OFF Switching: Rational Design, Synthesis, Optical Properties, Theoretical Calculations, and Applications for Fluorescence Imaging in Living Animals. *J. Am. Chem. Soc.* **2012**, *134*, 1200-1211.

(22) Karton-Lifshin, N.; Segal, E.; Omer, L.; Portnoy, M.; Satchi-Fainaro, R.; Shabat, D. A Unique Paradigm for a Turn-ON Near-Infrared Cyanine-Based Probe: Noninvasive Intravital Optical Imaging of Hydrogen Peroxide. *J. Am. Chem. Soc.* **2011**, *133*, 10960-10965.

(23) Chai, X.; Xiao, J.; Li, M.; Wang, C.; An, H.; Li, C.; Li, Y.; Zhang, D.; Cui, X.; Wang, T. Bridge-Caging Strategy in Phosphorus-Substituted Rhodamine for Modular Development of Near-Infrared Fluorescent Probes. *Chem. Eur. J.* **2018**, *24*, 14506–14512.

(24) Chen, W.; Xu, S.; Day, J. J.; Wang, D.; Xian, M. A General Strategy for Development of Near-Infrared Fluorescent Probes for Bioimaging. *Angew. Chem. Int. Ed.* **2017**, *129*, 16838-16842.

(25) Shuhendler, A. J.; Pu, K.; Cui, L.; Uetrecht, J. P.; Rao, J. Real-Time Imaging of Oxidative and Nitrosative Stress in the Liver of Live Animals for Medicine-Toxicity Testing. *Nat. Biotechnol.* **2014**, *32*, 373-380.

(26) Peng, J.; Samanta, A.; Zeng, X.; Han, S.; Wang, L.; Su, D.; Loong, D. T. B.; Kang, N.-Y.; Park, S.-J.; All, A. H.; Jiang, W.; Yuan, L.; Liu, X.; Chang, Y.-T. Real-Time in Vivo Hepatotoxicity Monitoring through Chromophore-Conjugated Photon-Upconverting Nanoprobes. *Angew. Chem. Int. Ed.* **2017**, *56*, 4165-4169.

(27) He, X.; Li, L.; Fang, Y.; Shi, W.; Li, X.; Ma, H. In Vivo Imaging of Leucine Aminopeptidase Activity in Medicine-Induced Liver Injury and Liver Cancer via a Near-Infrared Fluorescent Probe. *Chem. Sci.* **2017**, *8*, 3479-3483.

(28) Oushiki, D.; Kojima, H.; Terai, T.; Arita, M.; Hanaoka, K.; Urano, Y.; Nagano, T. Development and Application of a Near-Infrared Fluorescence Probe for Oxidative Stress Based on Differential Reactivity of Linked Cyanine Dyes. *J. Am. Chem. Soc.* **2010**, *132*, 2795-2801.

(29) Xu, W.; Teoh, C. L.; Peng, J.; Su, D.; Yuan, L.; Chang, Y.-T. A Mitochondria-Targeted Ratiometric Fluorescent Probe to Monitor Endogenously Generated Sulfur Dioxide Derivatives in Living Cells.

Biomaterials **2015**, *56*, 1-9.

(30) Yuan, L.; Kaplowitz, N. Mechanisms of Medicine-Induced Liver Injury. *Clin. Liver Dis.* **2013**, *17*, 507-518.

(31) Shi, Q.; Hong, H.; Senior, J.; Tong, W. Biomarkers for Medicine-Induced Liver Injury. *Expert Rev. Gastroenterol. Hepatol.* **2010**, *4*, 225-234.

(32) Amacher, D. E.; Schomaker, S. J.; Aubrecht, J. Development of Blood Biomarkers for Medicine-Induced Liver Injury: an Evaluation of Their Potential for Risk Assessment and Diagnostics. *Mol. Diagn. Ther.* **2013**, *17*, 343-354.

(33) Aithal, G. P.; Watkins, P. B.; Andrade, R. J.; Larrey, D.; Molokhia, M.; Takikawa, H.; Hunt, C. M.; Wilke, R. A.; Avigan, M.; Kaplowitz, N.; Bjornsson, E.; Daly, A. K. Case Definition and Phenotype Standardization in Medicine-Induced Liver Injury. *Clin. Pharmacol. Ther.* **2011**, *89*, 806-815.

(34) Lee, W. M. Acetaminophen (APAP) Hepatotoxicity-Isn't It Time for APAP to Go Away? *J. Hepatol.* **2017**, *67*, 1324-1331.

(35) Han, D.; Shinohara, M.; Ybanez, M. D.; Saberi, B.; Kaplowitz, N. Adverse Medicine Reactions. *Springer-Verlag Berlin Heidelberg*, **2010**, 267.

(36) Szabo, C.; Ischiropoulos, H.; Radi, R. Peroxynitrite: Biochemistry, Pathophysiology and Development of Therapeutics. *Nat. Rev. Medicine Discov.* **2007**, *6*, 662-680.

(37) Pacher, P.; Beckman, J. S.; Liaudet, L. Nitric Oxide and Peroxynitrite in Health and Disease. *Physiol. Rev.* **2007**, *87*, 315-424.

(38) (a) Mericas, G.; Anagnostou, E.; Hadziyannis, S.; Kakari, S. The Diagnostic Value of Serum Leucine Aminopeptidase. *J. Clin. Path.* **1964**, *17*, 52-55. (b) Banks, B. M.; Pineda, E. P.; Goldbarg, J. A.; Rutenburg, A. M. Clinical Value of Serum Leucine Aminopeptidase Determinations. *New Engl. J. Med.* **1960**, *263*, 1277-1281.

(39) Pessayre, D.; Mansouri, A.; Berson, A.; Fromenty, B. Mitochondrial Involvement in Medicine-Induced Liver Injury. *Handb. Exp. Pharmacol.* **2010**, *196*, 311–365.

(40) Cheng, D.; Xu, W.; Yuan, L.; Zhang, X. Investigation of Medicine-Induced Hepatotoxicity and Its Remediation Pathway with Reaction-Based Fluorescent Probes. *Anal. Chem.* **2017**, *89*, 7693-7700.

(41) Kondo, C.; Shibata, K.; Terauchi, M.; Kajiyama, H.; Ino, K.; Nomura, S.; Nawa, A.; Mizutani, S.;

Kikkawa, F. A Novel Role for Placental Leucine Aminopeptidase (P-LAP) As a Determinant of Chemoresistance in Endometrial Carcinoma Cells. *Int. J. Cancer* **2006**, *118*, 1390-1394.

(42) Li, Y.; Xie, X.; Yang, X.; Li, M.; Jiao, X.; Sun, Y.; Wang, X.; Tang, B. Two-Photon Fluorescent Probe for Revealing Medicine-Induced Hepatotoxicity via Mapping Fluctuation of Peroxynitrite. *Chem. Sci.* **2017**, *8*, 4006-4011.

(43) Peng, T.; Chen, X.; Gao, L.; Zhang, T.; Wang, W.; Shen, J.; Yang, D. A Rationally Designed Rhodamine-Based Fluorescent Probe for Molecular Imaging of Peroxynitrite in Live Cells and Tissues. *Chem. Sci.* **2016**, *7*, 5407-5413.

(44) Sun, Q.; Yang, S.-H.; Wu, L.; Dong, Q.-J.; Yang, W.-C.; Yang, G.-F. Detection of Intracellular Selenol-Containing Molecules Using a Fluorescent Probe with Near-Zero Background Signal. *Anal. Chem.* **2016**, *88*, 6084-6091.

(45) Feng, S.; Liu, D.; Feng, W.; Feng, G. Allyl Fluorescein Ethers as Promising Fluorescent Probes for Carbon Monoxide Imaging in Living Cells. *Anal. Chem.* **2017**, *89*, 3754-3760.

(46) Burley, S. K.; David, P. R.; Lipscomb, W. N. Leucine Aminopeptidase: Bestatin Inhibition and a Model for Enzyme-Catalyzed Peptide Hydrolysis. *Proc. Natl. Acad. Sci. USA* **1991**, *88*, 6916-6920.

(47) Knight, T. R.; Kurtz, A.; Bajt, M. L.; Hinson, J. A.; Jaeschke, H. Vascular and Hepatocellular Peroxynitrite Formation during Acetaminophen Toxicity: Role of Mitochondrial Oxidant Stress. *Toxicol. Sci.* **2001**, *62*, 212-220.

(48) Muijsers, R. B. R.; van den Worm, E.; Folkerts, G.; Beukelman, C. J.; Koster, A. S.; Postma, D. S.; Nijkamp, F. P. Apocynin Inhibits Peroxynitrite Formation by Murine Macrophages. *Brit. J. Pharmacol.* **2000**, *130*, 932-936.

(49) Xu, Z.; Xu, L. Fluorescent Probes for the Selective Detection of Chemical Species inside Mitochondria. *Chem. Commun.* **2016**, *52*, 1094-1119.

(50) Dickinson, B. C.; Srikun, D.; Chang, C. J. Mitochondrial-Targeted Fluorescent Probes for Reactive Oxygen Species. *Curr. Opin. Chem. Biol.* **2010**, *14*, 50-56.

(51) Cover, C.; Mansouri, A.; Knight, T. R.; Bajt, M. L.; Lemasters, J. J.; Pessayre, D.; Jaeschke, H. Peroxynitrite-Induced Mitochondrial and Endonuclease-Mediated Nuclear DNA Damage in Acetaminophen Hepatotoxicity. *J. Pharmacol. Exp. Ther.* **2005**, *315*, 879-887.

(52) He, C.; Liang, B.; Fan, X.; Cao, L.; Chen, R.; Guo, Y.; Zhao, J. The Dual Role of Osteopontin in

Acetaminophen Hepatotoxicity. *ActaPharmacol. Sin.* **2012**, *33*, 1004-1012.

(53) Gregory, S.; Kelly, N. D. Clinical Applications of N-acetylcysteine. *Alt. Med. Rev.* **1998**, *3*, 114-127.

(54) Chalasani, N. P.; Hayashi, P. H.; Bonkovsky, H. L.; Navarro, V. J.; Lee, W. M.; Fontana, R. J. ACG Clinical Guideline: the Diagnosis and Management of Idiosyncratic Medicine-Induced Liver Injury. *Am. J. Gastroenterol.* **2014**, *109*, 950-966.

(55) Yin, L.; Wei, L.; Fu, R.; Ding, L.; Guo, Y.; Tang, L.; Chen, F. Antioxidant and Hepatoprotective Activity of Veronica ciliate Fisch. Extracts Against Carbon Tetrachloride-Induced Liver Injury in Mice. *Molecules* **2014**, *19*, 7223-7236.

(56) OzelCoskuna, B. D.; Yucesoya, M.; Gursoya, S.; Baskola, M.; Yurcia, A.; Yagbasana, A.; Doğanb, S.; Baskol, G. Effects of Ursodeoxycholic Acid Therapy on Carotid Intima Media Thickness, Apolipoprotein A1, Apolipoprotein B, and Apolipoprotein B/A1 Ratio in Nonalcoholic Steatohepatitis. *Eur. J. Gastroenterol. Hepatol.* **2015**, *27*, 142-149.

(57) Liu, J.; Sun, Y.-Q.; Zhang, H.; Shi, H.; Shi, Y.; Guo, W. Sulfone-Rhodamines: A New Class of Near-Infrared Fluorescent Dyes for Bioimaging. *ACS Appl. Mater. Interfaces* **2016**, *8*, 22953-22962.

TOC:

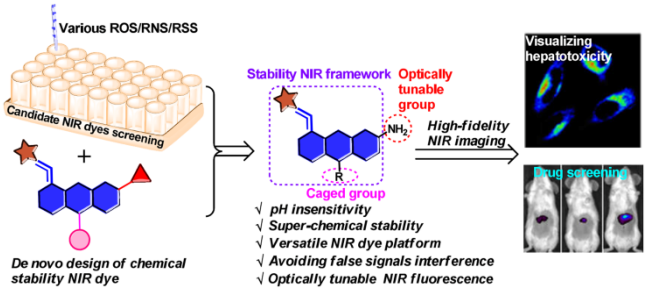
Various ROS/RNS/RSS
Candidate NIR dyes screening
De novo design of chemical stability NIR dye
Stability NIR framework
Optically tunable group
Caged group
√ pH insensitivity
√ Super-chemical stability
√ Versatile NIR dye platform
√ Avoiding false signals interference
√ Optically tunable NIR fluorescence
High-fidelity NIR imaging
Visualizing hepatotoxicity
Drug screening